Since January 2020 Elsevier has created a COVID-19 resource centre with free information in English and Mandarin on the novel coronavirus COVID-19. The COVID-19 resource centre is hosted on Elsevier Connect, the company's public news and information website.

Antiviral Research 208 (2022) 105445

Contents lists available at ScienceDirect

Antiviral Research

journal homepage: www.elsevier.com/locate/antiviral

Potent inhibition of diverse Omicron sublineages by SARS-CoV-2 fusion-inhibitory lipopeptides

Yuanmei Zhu [1], Yue Hu [1], Nian Liu [1], Huihui Chong, Yuxian He [*]

NHC Key Laboratory of Systems Biology of Pathogens, Institute of Pathogen Biology and Center for AIDS Research, Chinese Academy of Medical Sciences and Peking Union Medical College, Beijing, 100730, China

ARTICLE INFO

Keywords:
SARS-CoV-2
Variants of concern
Omicron sublineages
Fusion inhibitor
Lipopeptide

ABSTRACT

The emergence and rapid spreading of SARS-CoV-2 variants of concern (VOCs) have posed a great challenge to the efficacy of vaccines and therapeutic antibodies, calling for antivirals that can overcome viral evasion. We recently reported that SARS-CoV-2 fusion-inhibitory lipopeptides, IPB02V3 and IPB24, possessed the potent activities against divergent VOCs, including Alpha, Beta, Gamma, Delta, and the initial Omicron strain (B.1.1.529); however, multiple Omicron sublineages have emerged and BA.4/5 is now becoming predominant globally. In this study, we focused on characterizing the functionality of the spike (S) proteins derived from Omicron sublineages and their susceptibility to the inhibition of IPB02V3 and IPB24. We first found that the S proteins of BA.2, BA.2.12.1, BA.3, and BA.4/5 exhibited significantly increased cell fusion capacities compared to BA.1, whereas the pseudoviruses of BA.2.12.1, BA.3, and BA.4/5 had significantly increased infectivity relative to BA.1 or BA.2. Next, we verified that IPB02V3 and IPB24 also maintained their very high potent activities in inhibiting diverse Omicron sublineages, even with enhanced potencies relative to the inhibition on ancestral virus. Moreover, we demonstrated that evolved Omicron mutations in the inhibitor-binding heptad repeat 1 (HR1) site could impair the S protein-driven cell fusogenicity and infectivity, but none of single or combined mutations affected the antiviral activity of IPB02V3 and IPB24. Therefore, we believe that viral fusion inhibitors possess high potential to be developed as effective drugs for fighting SARS-CoV-2 variants including diverse Omicron sublineages.

1. Introduction

The global COVID-19 pandemic has lasted for nearly three years and caused more than 6 million death cases (https://covid19.who.int/). During its persistence, many SARS-CoV-2 variants emerged and led to successive waves of infection. In November 2021, Omicron variant (B.1.1.529) was reported as the fifth variant of concern (VOC) after Alpha (B.1.1.7) and Beta (B.1.351), Gamma (P1), and Delta (B.1.617.2), being characterized with higher transmissibility and immune evasion (Kuzmina et al., 2021; Hoffmann et al., 2021; Garcia-Beltran et al., 2021; Callaway, 2021; He et al., 2020; Guo et al., 2022; Markov et al., 2022). Genome-sequencing data indicate that Omicron evolves with the largest number of mutations and can be classified into distinct sublineages: BA.1 was responsible for the initial surge but almost replaced by BA.2 in April 2022; while BA.3, which carries a mosaic of BA.1 and BA.2 changes, is at a very low frequency, BA.4 and BA.5 are expected to replace BA.2 becoming prevalent worldwide (Tegally et al., 2022; Qu et al., 2022). As illustrated in Fig. 1, BA.4 and BA.5 possess identical spike (S) protein sequences, appear to have evolved from BA.2, but they contain additional Δ67–70, L452R, and F486V mutations and a wild type amino acid at position Q493, which critically determine their increased fitness and resistance to antibody neutralization than the earlier BA.1 and BA.2 sublineages (Cao et al., 2022). The emergence and rapid spreading of BA.4/5 have posed a great challenge to the efficacy of preventive vaccines and therapeutic antibodies, calling for urgent development of potent, broad-spectrum antivirals.

SARS-CoV-2 infection is mediated by its surface S protein through either a cell surface plasma or endosomal membrane fusion pathway, in which N-terminal S1 subunit is responsible for receptor binding and C-terminal S2 subunit mediates membrane fusion (Wrapp et al., 2020; Walls et al., 2020). Peptides derived from the heptad repeat 1 (HR1) or 2 (HR2) domains of viral fusion proteins can competitively block the

* Corresponding author.
E-mail address: yhe@ipb.pumc.edu.cn (Y. He).
[1] These authors contributed equally to this work.

https://doi.org/10.1016/j.antiviral.2022.105445
Received 22 August 2022; Received in revised form 3 October 2022; Accepted 10 October 2022
Available online 17 October 2022

formation of a six-helical HR1-HR2 bundle (6-HB) structure, which is essential to juxtapose the viral and cell membranes for merging (Tang et al., 2020; Zhu et al., 2020). In the outbreak of COVID-19, we quickly developed a group of lipopeptide-based fusion inhibitors with the HR2 sequences, including IPB02V3 and IPB24 (Zhu et al., 2020, 2021; Yu et al., 2021a, 2021b). Very recently, we reported that IPB02V3 and IPB24 possessed the highly potent activity against divergent VOVs and related mutants (Zhu et al., 2022). Considering that we are currently working to develop a lipopeptide for clinical use, it is fundamentally important to characterize Omicron sublineages for their cell fusion capacity, infectivity and susceptibility to the fusion inhibitors that we developed. In this study, we first analyzed the functionality of S proteins derived from several Omicron sublineages; then, the inhibitory activities of IPB02V3 and IPB24 on S protein-driven cell fusion and pseudovirus infection were evaluated. Furthermore, we explored the impacts of evolved Omicron HR1 mutations on virus's infectivity and antiviral activity of the fusion inhibitor lipopeptides.

2. Materials and methods

2.1. Plasmids, cells and inhibitors

Plasmids encoding the S proteins of the ancestral SARS-CoV-2 (Wuhan-Hu-1) and various Omicron sublineages (BA.1 and BA.2, not BA.2.12.1, BA.3, and BA.4/5) were kindly provided by Linqi Zhang at the Tsinghua University (Beijing, China). Plasmids encoding DSP_{1-7} and DSP_{8-11} were kindly provided by Zene Matsuda at the Institute of Medical Science of the University of Tokyo (Tokyo, Japan). 293T/ACE2 cells stably expressing human ACE2 were produced and preserved in our laboratory. 293T and Huh-7 cells were purchased from the American type culture collection (ATCC) (Rockville, MD, USA). Cells were cultured in complete growth medium contained Dulbecco's minimal essential medium (DMEM), 10% fetal bovine serum (FBS), 100 U/ml of penicillin-streptomycin, 2 mM L-glutamine, and 1 mM sodium pyruvate under 37 °C and 5% CO_2. IPB02V3 and IPB24 lipopeptides were generated from our previous studies (Zhu et al., 2021; Yu et al., 2021a).

2.2. Cell-cell fusion assay

The S protein-mediated cell-cell fusion activity was determined by a dual-split-protein (DSP)-based cell-cell fusion assay as described previously (Zhu et al., 2020). A total of 1.5×10^4 293T cells were seeded in a 96-well plate as effector cells; 1.5×10^5/ml 293T/ACE2 cells were cultured in a 10-cm culture dish as target cells. After culturing at 37 °C overnight, effector cells were cotransfected with a mixture of a plasmid expressing S protein (0.1 μg) and a DSP_{1-7} plasmid (0.1 μg), whereas target cells were transfected with a DSP_{8-11} plasmid (24 μg), followed by incubation at 37 °C for 24 h. To measure the inhibitory activity of IPB02V3 or IPB24, a serially 3-fold diluted lipopeptide was added to the effector cells and incubated for 1 h, whereas the target cells were resuspended at 3×10^5/ml in prewarmed culture medium containing ~17 ng/ml EnduRen live cell substrate (Promega, Madison, WI, USA)

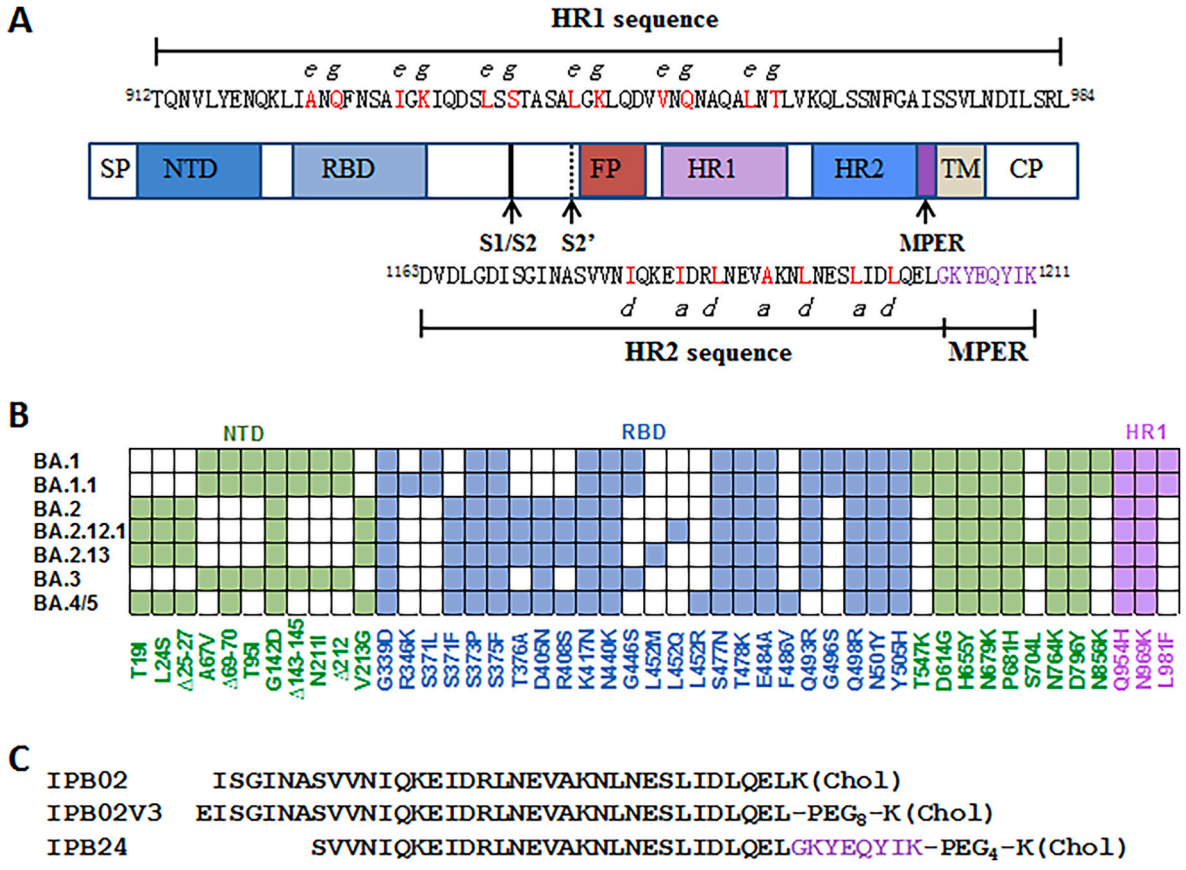

Fig. 1. Schematic diagram of SARS-CoV-2 S protein and fusion inhibitors. (**A**) Functional domains of the S protein and HR1/HR2 sequences. SP, signal peptide; NTD, N-terminal domain; RBD, receptor-binding domain; FP, fusion peptide; HR1, heptad repeat 1 region; HR2, heptad repeat 2 region; MPER, membrane-proximal external region; TM, transmembrane domain; CP, cytoplasmic peptide. The S1/S2 and S2′ cleavage sites and MPER are marked with arrow. The HR1 and HR2 core sequences as well as the MPER sequence are listed, in which the potential residues that mediate the HR1-HR2 interactions in 6-HB are colored in red. (**B**) Illustration of mutations on the S protein of Omicron sublineages. Residues that are not identical among Omicron sublineages are colored green, blue or purple for clarity. (**C**) Representative fusion-inhibitory lipopeptides based on the HR2-MPER sequences. The MPER amino acids are colored in purple. Chol, cholesterol; PEG8 or PEG4, 8-unit or 4-unit polyethylene glycol.

and incubated for 30 min. Then, 3×10^4 of target cells were transferred to the effector cells, and the cell mixtures were spun down to promote cell-cell contact. Luciferase activity was measured at different time points using luciferase assay reagents and a luminescence counter (Promega).

2.3. Single-cycle infection assay

Infectivity of diverse SARS-CoV-2 Omicron pseudoviruses in 293T/ACE2 or Huh-7 cells was determined by a single-cycle infection assay as described previously (Yu et al., 2021a). To generate a pseudovirus, 5×10^6 of 293T cells grown in 15 ml of growth medium in a T-75 culture flask were cotransfected with 10 μg of S protein-expressing plasmids and 20 μg of lentivral backbone plasmids (pNL4-3.luc.RE) encoding an Env-defective, luciferase reporter-expressing HIV-1 genome. After 48 h culture, cell supernatants containing released pseudoviruses were collected, filtrated and stored at −80 °C. The 50% tissue culture infectious dose ($TCID_{50}$) of pseudovirus was determined in 293T/ACE2 and Huh-7 cells. To compare the infection capacities of pseudoviruses, viral particles were normalized to a fixed amount by p24 antigen at 20 ng, and their relative infectivity was calculated. To measure the inhibitory activity of IPB02V3 or IPB24, a serially 3-fold diluted lipopeptide was incubated with an equal volume of pseudoviruses (500 $TCID_{50}$) at 37 °C for 30 min, and the virus-inhibitor mixture was then added to 10^4 cells/well of target cells (293T/ACE2 or Huh-7). After incubation at 37 °C for 48 h, the cells were harvested and lysed in reporter lysis buffer (Promega), followed by the measurement of luciferase activity as described above.

2.4. Site-directed mutagenesis

S protein mutants were generated by site-directed mutagenesis as described previously (Yu et al., 2021a). In brief, the forward and reverse primers with 16–28 nucleotides were designed with desired mutations and occupied the same starting and ending positions on the opposite strands of a codon-optimized S gene cloned in a pcDNA3.1 vector. DNA synthesis was conducted by PCR in a 50-μl reaction volume using 100 ng of denatured plasmid template, 50 pM upper and lower primers, and 5 U of the high-fidelity polymerase PrimeStar (TaKaRa, Dalian, China). PCR amplification was done for one cycle of denaturation at 98 °C for 5 min, followed by 25 cycles of 98 °C for 10 s and 68 °C for 9 min, with a final extension at 72 °C for 10 min. The amplicons were treated with restriction enzyme DpnI for 3 h at 37 °C, and DpnI-resistant molecules were recovered by transforming *E. coli* stable3 competent cells with antibiotic resistance. The required mutations were confirmed by DNA sequencing of a single clone.

2.5. Western blotting assay

The expression of various S proteins in cells were examined by Western blotting analysis. In brief, 5×10^5/ml 293T cells were seeded in a 12-well plate and transfected by S protein-encoding plasmids. After 48 h, transfected cells were harvested and lysed for 30 min on ice, followed by centrifugation (12,000×*g*) at 4 °C for 1h to remove insoluble materials. The supernatant of lysates was fixed to a same protein concentration by BCA Protein Assay Kit (Thermo Scientific, Rockford, IL, USA). Proteins in lysates were separated by SDS-PAGE and transferred to a nitrocellulose membrane. After blocking by 5% nonfat dry milk solution in Tris-buffered saline (TBS, pH 7.4) at room temperature for 1 h, the membrane was washed and then incubated with a rabbit anti-S1 or anti-S2 polyclonal antibody (SinoBiological, Beijing, China) overnight at 4 °C. On the following day, the membrane was washed and then incubated with IRDye 680LT goat-anti-rabbit IgG at room temperature for 2 h. β-actin was detected with a mouse anti-β-actin monoclonal antibody (Sigma, St. Louis, MO, USA) and IRDye 680LT donkey-anti-mouse IgG. The membrane was then scanned using the Odyssey infrared imaging system (LI-COR Biosciences, Lincoln, NE, USA).

2.6. Statistical analysis

Percent inhibition and 50% inhibitory concentration (IC_{50}) of tested inhibitors were calculated using GraphPad Prism 6 software (GraphPad Software Inc., San Diego, CA, USA). The comparisons of S protein-mediated cell-cell fusion activities and pseudovirus infections were conducted by one-way ANOVA with Dunnett's multiple comparisons test (ns, not significant; *, $p < 0.05$; **, $p < 0.01$; ***, $p < 0.001$; ****, $p < 0.0001$), in which $p < 0.05$ is considered as a significant difference.

3. Results

3.1. Functional characterization of S proteins derived from diverse Omicron sublineages

In order to characterize the functionality of S proteins from Omicron sublineages, we first applied a DSP-based cell fusion assay to determine the S protein-mediated cell-cell fusion activity. As shown in Fig. 2, the S proteins of BA.1 and BA.2, but not BA.2.12.1, BA.3, and BA.4/5, exhibited decreased cell fusion activities compared to the S protein of ancestral Wuhan-Hu-1 strain (WT); however, BA.2, BA.2.12.1, BA.3, and BA.4/5 had significantly increased fusion capacities relative to the BA.1 strain. The western blotting assays with both anti-S1 and anti-S2 antibodies showed that the WT and various Omicron S proteins had comparable expression levels in transfected cells (Fig. 2C), implying that the fusogenic differences were not directly caused by the overexpression system. There were minor changes observed on the S1 and S2 expression, but it was difficult to judge that they were due to an intrinsic cleavage effect or epitopic drift of the antibodies used, given that Omicron evolved with huge mutations throughout the S protein sequences.

Next, we conducted a pseudovirus-based single-cycle infection assay to measure the capacity of S protein to mediate viral infection. Comparing to WT, BA.1 and BA.2 infected both 293T/ACE2 and Huh-7 cells with reduced activities, BA.2.12.1 exhibited increased infectivity on 293T/ACE2 but decreased on Huh-7 cells, BA.3 showed reduced infection on Huh-7 cells only, whereas BA.4/5 significantly enhanced the infectivity on both of the cells (Fig. 3). In contrast, the cell entry capacities of BA.2.12.1, BA.3, and BA.4/5 were significantly higher than BA.1 or BA.2. When BA.2.12.1 was used as a reference, BA.3 exhibited reduced infection, whereas BA.4/5 remained the higher infectivity. Taken together, these results have indicated that BA.4/5 is more infectious than the WT strain and any of other Omicron subvariants. Nonetheless, when being compared to the ancestral Wuhan-Hu-1 strain with a single D614G mutation (D614G reference), which emerged with increased infectivity (Li et al., 2020; Korber et al., 2020), the S proteins of all the Omicron sublineages had significantly decreased activities to mediate the cell fusion and infection, except for the BA4/5 pseudovirus showing similar infectivity in 293T/ACE2 cells (Fig. 3C).

3.2. Lipopeptide fusion inhibitors maintain high potency against diverse Omicron sublineages

We next focused on investigating the activities of fusion-inhibitory lipopeptides IPB02V3 and IPB24 on diverse Omicron sublineages. First, their inhibitory activities against S protein-mediated cell-cell fusion were assessed by the DSP-based cell-cell fusion assay. As shown in Fig. 4(A) and Table 1, IPB02V3 and IPB24 potently blocked the cell fusion mediated by various Omicron S proteins. Specifically, IPB02V3 dose-dependently blocked BA.1, BA.2, BA.2.12.1, BA.3, and BA.4/5 with mean IC_{50} values of 0.28, 0.36, 0.4, 0.55, and 0.5 nM, respectively, whereas IPB24 dose-dependently blocked their fusions with the IC_{50} values of 0.18, 0.28, 0.3, 0.44, and 0.42 nM, respectively. Subsequently, we measured the inhibitory activities of IPB02V3 and IPB24 against the S protein-driven pseudoviruses by the single-cycle infection assay. As

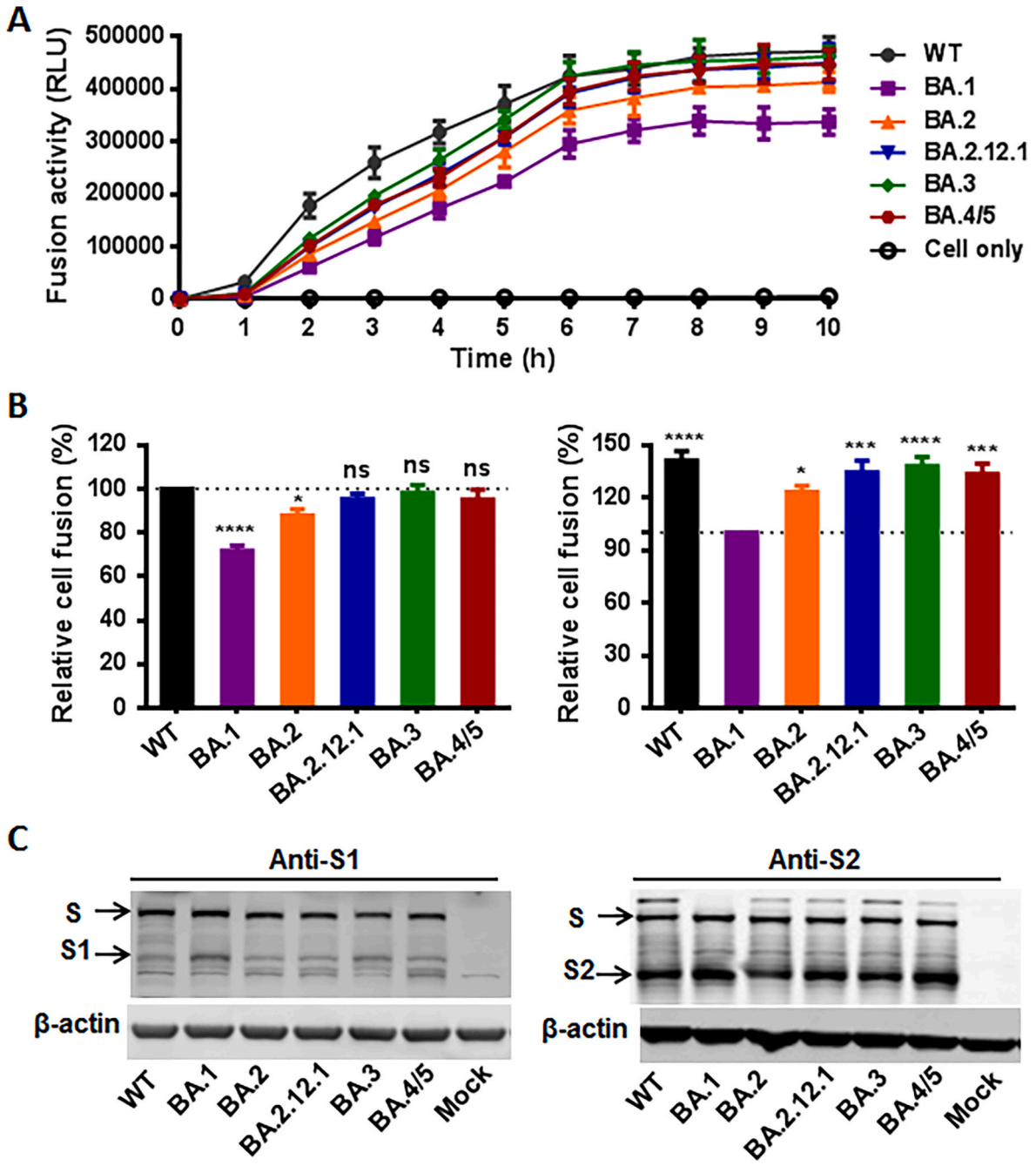

Fig. 2. Fusogenicity of diverse SARS-CoV-2 Omicron sublineages. (A) Fusion kinetics of divergent Omicron S proteins in 293T/ACE2 cells was determined at different time points by a DSP-based cell fusion assay. **(B)** The relative fusion activities of divergent Omicron S proteins at 8 h postfusion were calculated with wild-type (WT) (left panel) or BA.1 (right panel) as a reference. Data were derived from the results of three independent experiments and are expressed as means with standard deviations (SD). **(C)** The expression of various S proteins was analyzed by a western blotting assay, in which a rabbit anti-S1 (left panel) or anti-S2 (right panel) was used for detection.

shown by Fig. 4(B and C) and Table 1, the results also verified the potent activities of the lipopeptides against the infections of diverse Omicron sublineages. IPB02V3 respectively inhibited the BA.1, BA.2 BA.2.12.1, BA.3, and BA.4/5 pseudoviruses with IC_{50} of 4.69, 8.21, 5.64, 3.9, and 3.91 nM on 293T/ACE2 cells and with IC_{50} of 10.37, 7.4, 3.73, 4.75, and 4.68 nM on Huh-7 cells; IPB24 respectively inhibited the BA.1, BA.2 BA.2.12.1, BA.3, and BA.4/5 pseudoviruses with IC_{50} of 3.83, 0.91, 1.19, 0.98, and 1 nM on 293T/ACE2 cells and with IC_{50} of 2.24, 2.36, 1.56, 1.66, and 1.42 nM on Huh-7 cells. Comparing to the WT virus, the majority of Omicron sublineages, especially BA.4/5, appeared more sensentive to the inhibitions of two fusion-inhibitory lipopeptides.

3.3. Characterization of the impacts of specific HR1 mutations on viral fusion and inhibition

As illustrated in Fig. 1, BA.1 has evolved with three mutations (Q954H, N969K, L981F) in the inhibitor-binding HR1 site, whereas BA.2, BA.2.12.1, BA.3, and BA.4/5 possess two mutations (Q954H and N969K) only. Herein, we were intrigued to exploit the impacts of such substitutions on the S protein-driven cell fusion and pseudovirus infection as well as the inhibitory activities of IPB02V3 and IPB24. To this end, the S proteins bearing a point-mutation or combined mutations were generated by site-directed mutagenesis and used in the DSP-based

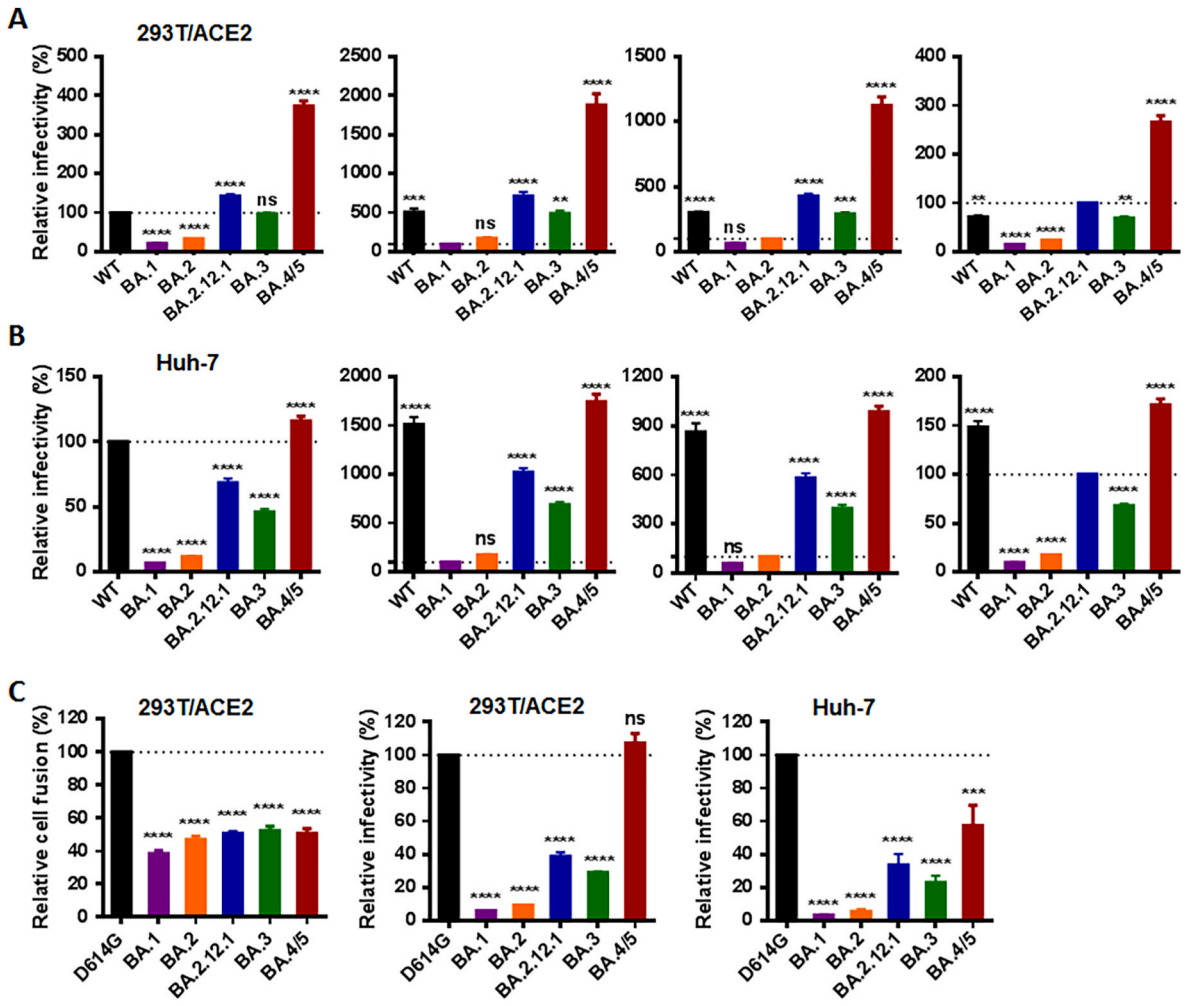

Fig. 3. Infectivity of diverse SARS-CoV-2 Omicron sublineages. The infectivity of S protein-pseudotyped Omicron sublineages was determined on 293T/ACE2 cells **(A)** and Huh-7 cells **(B)** by a single-cycle infection assay, in which the viral particles were normalized to a fixed amount by p24 antigen. In comparison, the luciferase activity (RLU) of WT, BA.1, BA.2, or BA.2.2.1 was treated as 100% (dotted lines) and the relative infectivity of other pseudoviruses was calculated accordingly. Data were derived from the results of three independent experiments and are expressed as means with SD. **(C)** The fusogenicity and infectivity of Omicron sublineages were compared to the D614G mutant as a reference.

cell fusion assay and single-cycle infection assay. Comparing to the background D614G reference, the S proteins with additional mutations of N969K, L981F, Q954H/N969K, or Q954H/N969K/L981F had significantly decreased fusogenic activities on both 293T/ACE2 and Huh-7 cells (Fig. 5(A)). Differently, while the pseudoviruses with the single Q954H mutation or triple Q954H/N969K/L981F mutations exhibited reduced infectivity on 293T/ACE2 cells, the single N969K mutant infected the cells with an enhanced capacity relative to the D614G reference. In Huh-7 cells, only the Q954H/N969K/L981F triple mutant was observed with reduced infectivity (Fig. 5(B)). Subsequently, we verified that none of the single or combined HR1 mutations negatively affected the inhibitory activities of IPB02V3 and IPB24 lipopeptides; instead, most mutants behaved with increased susceptibility to the inhibition by IPB02V3 (Fig. 5(C)).

4. Discussion

In this study we have finely characterized several Omicron sublineages for their cell fusogenicity, infectivity, and susceptibility to the inhibition of fusion inhibitors. First, we found that the S proteins of BA.1 and BA.2 sublineages exhibited significantly decreased fusogenicity relative to ancestral virus (WT), whereas the S proteins of BA.2, BA.2.12.1, BA.3, and BA.4/5 sublineages had significantly increased fusion activities than BA.1. As indicated by pseudoviruses, while BA.1 and BA.2 exhibited decreased infectivity on 293T/ACE2 and Huh-7 cells, BA.4/5 infected the two cells with a significantly capacity; but differently, BA.2.12.1 had increased infection on 293T/ACE2 but behaved with less infection on Huh-7 cells, whereas BA.3 displayed reduced infection on Huh-7 cells only. Comparing to the infectivity between the sublineages, BA.2.12.1, BA.3, and BA.4/5 were significantly higher than BA.1 and BA.2; while BA.3 exhibited reduced infectivity than BA.2.12.1, BA.4/5 remained the higher infectivity. Importantly, the results verified that IPB02V3 and IPB24 possessed their highly potent activities in inhibiting diverse Omicron S proteins-driven cell-cell fusion and pseudovirus infection. Furthermore, we also characterized the impacts of three evolved Omicron mutations in the spike HR1 site, and found that they attenuated the cell fusogenicity and infectivity, but none of the mutations affected the antiviral activities of IPB02V3 and IPB24 alone or in combinations. Therefore, here we conclude that viral fusion inhibitors possess a very potent, broad-spectrum activity against diverse Omicron subvariants; thus, IPB02V3 and IPB24 are ideal candidates for developing effective antivirals that overcome the problems of viral evasion and resistance.

The genetic evolution of SARS-CoV-2 has been extensively tracked since its sudden emergence in late December of 2019. Initially, a globally dominant variant with a single D614G mutation (D614G reference)

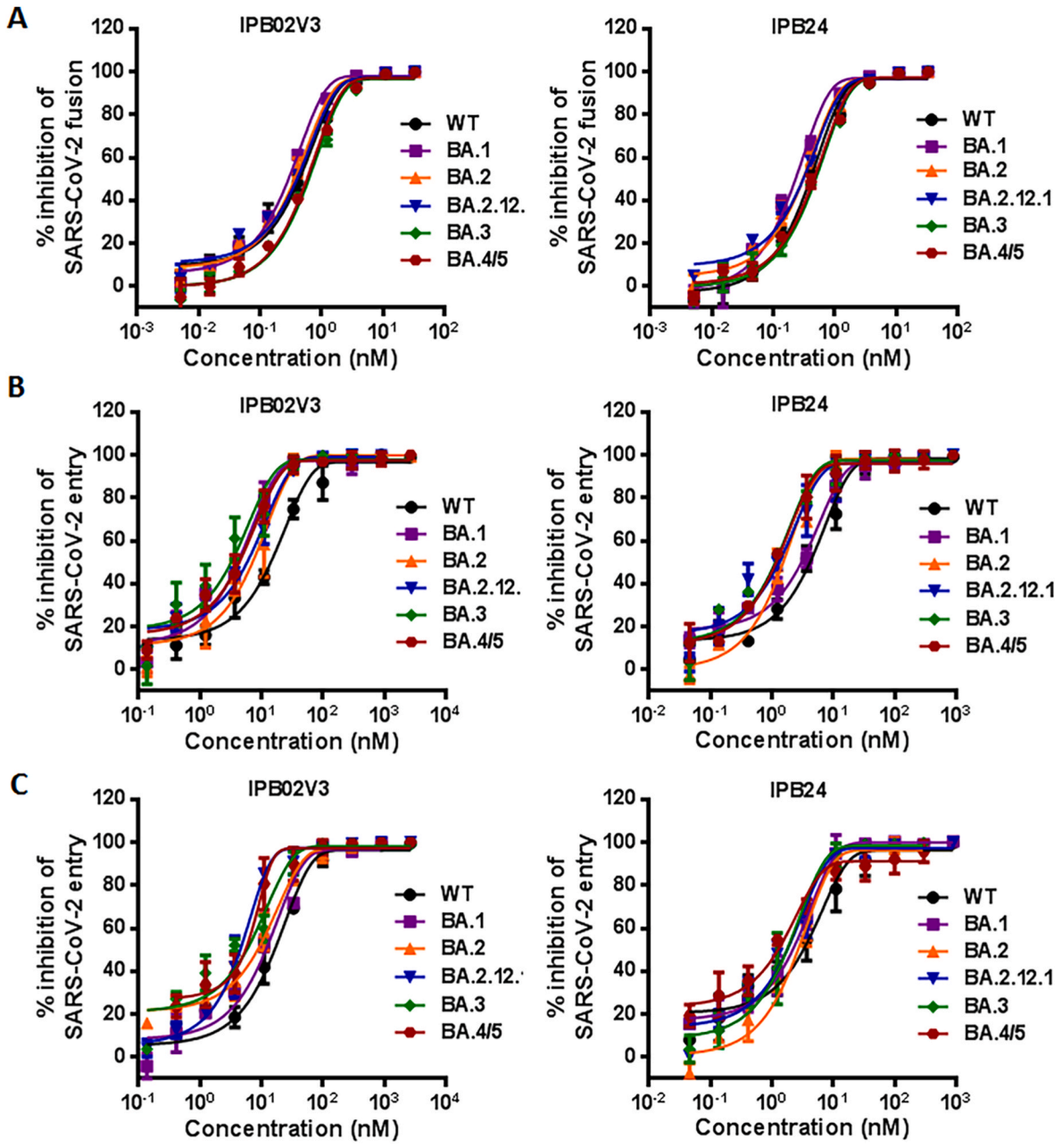

Fig. 4. Inhibitory activity of IPB02V3 and IPB24 against diverse Omicron sublineages. (A) The inhibitory activities of IPB02V3 and IPB24 against the Omicron S protein-driven cell-cell fusion were determined by a DSP-based cell fusion assay. The inhibitory activities of IPB02V3 and IPB24 against the infections of diverse Omicron pseudoviruses on 293T/ACE2 cells **(B)** and Huh-7 cells **(C)** were determined by a single-cycle infection assay. Samples were tested in triplicate, the experiments were repeated three times, and data are expressed as the means with SD.

Table 1
Inhibitory activity of lipopeptide fusion inhibitors against Omicron subvariants (IC_{50} ± SD, nM) [a].

SARS-CoV-2	Cell fusion		Pseudovirus on 293T/ACE2		Pseudovirus on Huh-7	
	IPB02V3	IPB24	IPB02V3	IPB24	IPB02V3	IPB24
WT	0.40 ± 0.05	0.34 ± 0.05	15.30 ± 0.76	4.09 ± 0.44	12.67 ± 2.48	2.74 ± 0.76
BA.1	0.28 ± 0.01***	0.18 ± 0.004***	4.69 ± 0.37****	3.83 ± 0.56	10.37 ± 1.96	2.24 ± 0.16
BA.2	0.36 ± 0.02*	0.28 ± 0.03	8.21 ± 3.11***	0.91 ± 0.47****	7.40 ± 1.41**	2.36 ± 0.27
BA.2.12.1	0.40 ± 0.04	0.30 ± 0.04	5.64 ± 0.05***	1.19 ± 0.23****	3.73 ± 0.52***	1.56 ± 0.51*
BA.3	0.55 ± 0.03**	0.44 ± 0.03**	3.90 ± 1.61****	0.98 ± 0.12****	4.75 ± 1.31***	1.66 ± 0.30*
BA.4/5	0.50 ± 0.02**	0.42 ± 0.04*	3.91 ± 0.95****	1.00 ± 0.18****	4.68 ± 1.36***	1.42 ± 0.23**

[a] The experiments were performed in triplicate and repeated three times, and data are expressed as the means ± SD. The inhibitory activities of IPB02V3 and IPB24 against diverse Omicron sublineages were statistically compared with that of the WT reference.

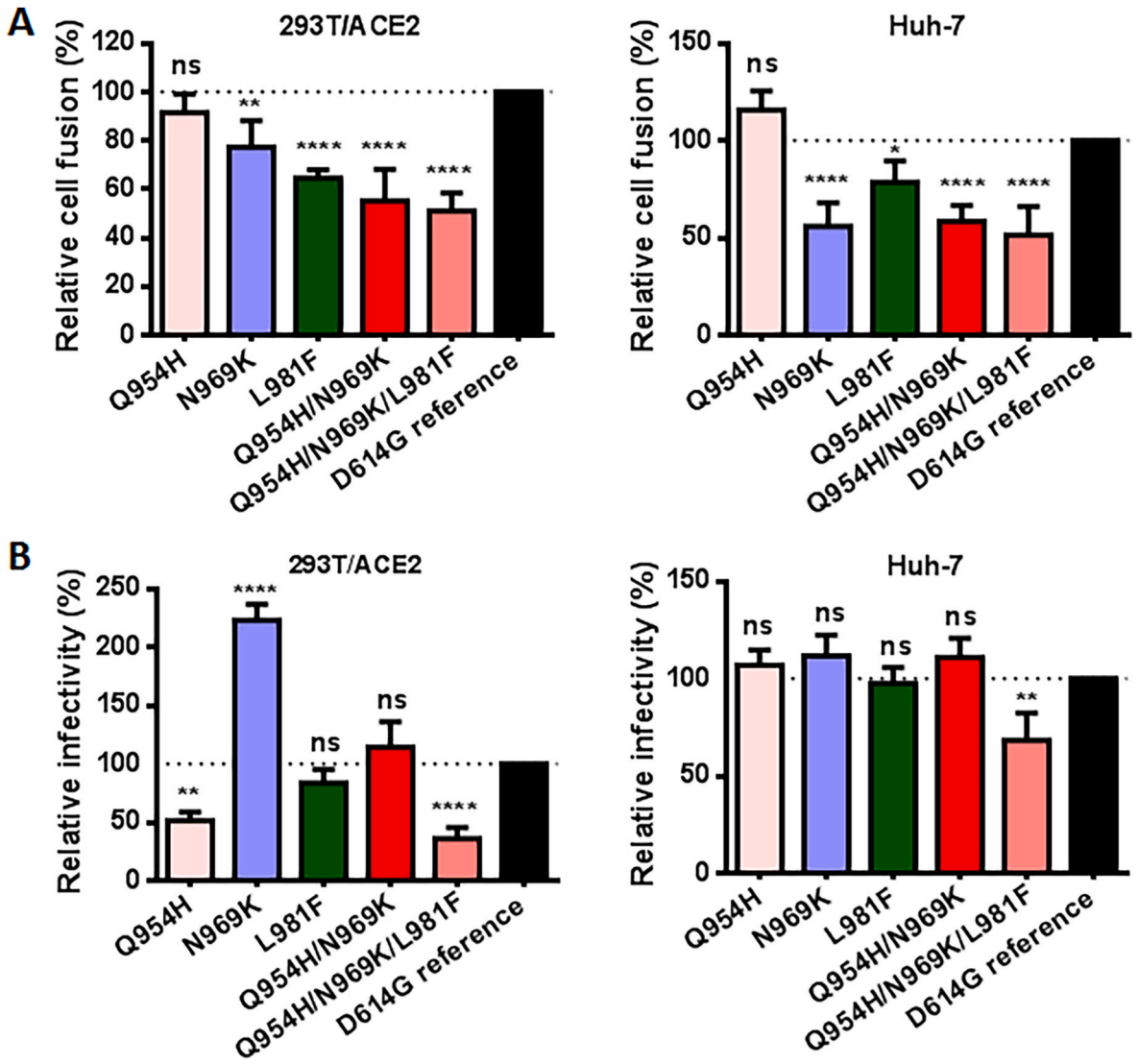

C

SARS-CoV-2	Pseudovirus on 293T/ACE2		Pseudovirus on Huh-7	
	IPB02V3	IPB24	IPB02V3	IPB24
D614G reference	15.17 ± 4.51	6.01 ± 1.84	13.23 ± 2.48	3.05 ± 1.13
Q954H	7.33 ± 0.81*	6.21 ± 1.79	6.39 ± 1.95**	4.09 ± 1.86
N969K	9.90 ± 3.87	3.15 ± 0.84	3.98 ± 0.93****	1.58 ± 0.62
L981F	16.06 ± 4.90	5.32 ± 0.60	6.03 ± 2.69***	1.82 ± 0.42
Q954H/N969K	8.04 ± 2.97*	4.08 ± 1.57	4.99 ± 0.78****	3.85 ± 1.33
Q954H/N969K/L981F	7.89 ± 2.14*	6.25 ± 2.68	7.03 ± 2.05**	5.34 ± 1.80

Fig. 5. Characterization of the impacts of Omicron HR1 mutations on the functionality of S protein and viral susceptibility to fusion-inhibitory lipopeptides. (A) The fusion capacities of S proteins with single or combined HR1 mutations in 293T/ACE2 cells (right panel) and Huh-7 cells (left panel) were measured by the DSP-based cell fusion assay, and the relative fusion activities of HR1 mutants were compared with the D614G reference. **(B)** The infectivity of pseudoviruses bearing the HR1 mutations in 293T/ACE2 cells (right panel) and Huh-7 cells (left panel) was measured by the single-cycle infection assay, and the relative activities of HR1 mutants were compared with the D614G reference. **(C)** The inhibitory activities of IPB02V3 and IPB24 against the pseudoviruses with HR1 mutations on 293T/ACE2 or Huh-7 cells were determined by the single-cycle infection assay. The IC_{50} values significantly lower than the D614G reference were marked in red. The experiments were repeated three times, and data are expressed as the means with SD.

was identified to be associated with the higher transmissibility but without increased disease severity of its ancestral strain (Korber et al., 2020). Since then, a large number of SARS-CoV-2 variants with the D614G background have been described, of which five are declared as VOCs, being associated with enhanced transmissibility or virulence, reduction in antibody neutralization, the ability to escape detection, or decrease in therapeutics or vaccination effectiveness. Following the Alpha, Beta, Gamma, and Delta variants, Omicron (B.1.1.529) was first

identified in South Africa on November 23, 2021 after an uptick in the number of COVID-19 cases; however, it has rapidly replaced Delta to become the globally dominant virus and caused a number of breakthrough infection or re-infection (He et al., 2020; Guo et al., 2022; Markov et al., 2022). Compared to the ancestral Wuhan-Hu-1 strain (WT), the S protein of Omicron B.1.1.529 contains more than 30 mutations, including the mutations in the N-terminal domain (A67V, H69del, V70del, T95I, G142D, Y143del, Y145del, Y144del, N211del/L212I), receptor-binding domain (G339D, S371L, S373P, S375F, K417N, N440K, G446S, S477N, T478K, E484A, Q493R, G496S, Q498R, Y505H, N501Y), fusion peptide (D796Y), and HR1 site (Q954H, N969K, L981F) (Callaway, 2021; He et al., 2020; Tao et al., 2021; Yamasoba et al., 2022). Previous studies reported that while the S proteins of Delta and other variants had enhanced fusogenicity and infectivity, the S protein of Omicron exhibited significantly reduced fusion activity (He et al., 2020; Zhu et al., 2022; Saito et al., 2022; Zhang et al., 2021; Zhao et al., 2022; Zeng et al., 2022). Very recently, Bowen and coauthors observed the slower and markedly reduced overall fusogenicity for all tested Omicron sublineages compared to the D614G reference (Wuhan-Hu-1/G614) (Bowen et al., 2022). Consistently, we previously showed that D614G reference had dramatically increased fusogenicity and infectivity, whereas B.1.1.529 displayed markedly decreased fusogenicity and infectivity relative to the D614G reference (Zhu et al., 2021, 2022). Herein, our results indicated that compared to the WT virus, only BA.1 and BA.2 sublineages, but not BA.2.12.1, BA.3, and BA.4/5, exhibited the S proteins with reduced fusogenicity; nonetheless, the fusion capacities of BA.2, BA.2.12.1, BA.3, and BA.4/5 were significantly enhanced relative to the BA.1 sublineage (Fig. 2). As demonstrated by pseudoviruses, Omicron sublineages had distinct infectivity, whereas BA.2.12.1 and BA.4/5 exhibited the enhanced infectivity than the earlier BA.1 and BA.2 sublineages; however, all tested Omicron sublineages sharply reduced the fusogenicity when compared to the D614G reference, in agreement with the results by Bowen et al. (2022). Taken together, our data have underscored the complexities of Omicron's membrane fusion that need to be addressed in detail. As we discussed previously, how Omicron evolves with reduced fusogenicity but behaves with dramatically increased transmissibility is an intriguing question (Zhu et al., 2022). Furthermore, it has been thought that the Omicron variant (relative to previously circulating VOCs) exhibits a shift from cell surface entry to endosomal entry. Herein, we wonder how Omicron pseudoviruses enter 293T/ACE2 or Huh-7 cells, which only allow for endosomal entry, with lower efficiency as compared to the particles bearing the WT or D614G spike (Fig. 3). Definitely, the mechanisms underlying the relationships between the viral fusogenicity, entrance pathway, infectivity, transmissibility and pathogenicity need be comprehensively investigated in future studies.

The failure of antibody therapy highlights the importance of antivirals that can overcome viral evasion and resistance. Emerging studies have demonstrated that fusion-inhibitory lipopeptides possess high antiviral activity and improved stability (Xue et al., 2022; Zhu et al., 2018, 2019; Chong et al., 2016, 2017, 2018a, 2018b, 2019; Ding et al., 2017). While a native HR2-derived peptide can block direct entrance from the cell surface but not entrance through endosomal pathway, lipopeptides also enables activity against viruses that do not fuse until they have been taken up via endocytosis (Ujike et al., 2008; Lee et al., 2011). In an immediate action to fight against COVID-19, we quickly characterized the fusogenicity of SARS-CoV-2 and accordingly designed a potent fusion-inhibitory lipopeptide termed IPB02 (Zhu et al., 2020). We further optimized the antiviral activity of IPB02 by introducing a flexible linker between the peptide sequence and lipid group, thus generating several lipopeptides with significantly improved activity, as represented by IPB02V3 (Zhu et al., 2021). Later, the spike membrane-proximal external region (MPER) was identified to be critical in viral fusogenicity and infectivity, and thus, we further designed lipopeptides containing the MPER sequence, as represented by IPB24 (Yu et al., 2021a). We previously showed that IPB24 possessed the potent activities against SARS-CoV-2 and the D614G reference, as well as the viruses bearing the S protein mutations of E484K, N501Y, Δ69–70, N501Y/Δ69–70/P681H, or N501Y/E484K/K417N (Yu et al., 2021a). We recently showed that both IPB02V3 and IPB24 were highly effective in inhibiting divergent VOCs, including Alpha, Beta, Gamma, Delta, and Omicron B.1.1.529 (Zhu et al., 2022). Again, the present studies verified that both the inhibitors maintained or even improved the activities in inhibiting diverse Omicron sublineages, thereby providing evidence to support the broad-spectrum activity of the fusion inhibitor-based antivirals. Moreover, three Omicron HR1 mutations (Q954H, N969K, and L981F) could also impair the S protein to mediate the cell fusion and infection alone or in combinations, but they did not affect the antiviral activities of IPB02V3 and IPB24. Several recent works also demonstrated the effectiveness of the lipopeptide-based fusion inhibitors against SARS-CoV-2 and its VOCs, despite only B.1.1.529 was tested in the studies (Schmitz et al., 2022; Xia et al., 2022; Lan et al., 2022). Additionally, two 5-helix-based and one HR2 trimer-based miniprotein fusion inhibitors also inhibited SARS-CoV-2 and its VOCs similarly but they exhibited much less potent activity overall (Xing et al., 2022; Lin et al., 2022; Bi et al., 2022). Collectively, it comes out with one more critical thinking: if the Omicron variant prefers endosomal entry over cell surface entry, why does not the shift affect the antiviral activity of fusion-inhibitory lipopeptides? Such inhibitors should exert more efficiently outside the targeting cells, whereas their intracellualr action requires the endocytosis process. As discussed above, an unconjugated, native HR2-derived peptide cannot effectively block the endosomal pathway because it is difficult to enter the cells. However, we have recently found that native HR2 peptides also exhibit similar or improved potencies in inhibiting Omicron sublineages in 293T/ACE2 and Huh-7 cells (unpublished data). Therefore, here we would like to emphasize that many efforts are required to elucidate the mechanisms of SARS-CoV-2 fusion/entry and its inhibition.

In one-sentence conclusion, we believe that SARS-CoV-2 fusion-inhibitory lipopeptides are ideal antivirals against divergent Omicron sublineages and other emerging or re-emerging variants, and hopefully, one of our lipopeptide-based drugs will be evaluated in clinical trials soon. Although the recent studies with authentic viruses have demonstrated that the initial Omicron variant is more susceptible than the WT strain and various variants to fusion-inhibitory lipopeptides (Zhu et al., 2022; Schmitz et al., 2022), it is still necessary to determine the potency and breadth of the lipopeptides against emerging Omicron sublineages with the *in virto* and *in vivo* replicative viruses. Indeed, we are in pocess to evaluate the inhibitors with different target cells and animal models, which will not only complement the presented data, but also facilitate the future clinical development.

Author contributions

Y.Z., Y.H., N.L., H.C. performed the experiments. Y.Z., Y.H. and Y.H. analyzed the data. Y.H. designed the study and wrote the paper.

Declaration of competing interest

The authors declare that they have no known competing financial interests or personal relationships that could have appeared to influence the work reported in this paper.

Data availability

Data will be made available on request.

Acknowledgements

We thank Linqi Zhang at the Tsinghua university (Beijing, China) for providing the plasmids encoding the S proteins of Omicron sublineages, and Zene Matsuda at the Institute of Medical Science, University of

Tokyo (Tokyo, Japan) for providing the DSP1-7 and DSP8-11 plasmids used in the cell fusion assay. This work was supported by grants from the CAMS Innovation Fund for Medical Sciences (2021-I2M-1037), and the National Natural Science Foundation of China (82221004, 82230076).

References

Bi, W., Chen, G., Dang, B., 2022. Novel engineered SARS-CoV-2 HR1 trimer exhibits improved potency and broad-spectrum activity against SARS-CoV-2 and its variants. J. Virol. 96, e0068122.

Bowen, J.E., Addetia, A., Dang, H.V., Stewart, C., Brown, J.T., Sharkey, W.K., et al., 2022. Omicron spike function and neutralizing activity elicited by a comprehensive panel of vaccines. Science, eabq0203.

Callaway, E., 2021. Heavily mutated Omicron variant puts scientists on alert. Nature 600, 21.

Cao, Y., Yisimayi, A., Jian, F., Song, W., Xiao, T., Wang, L., et al., 2022. BA.2.12.1, BA.4 and BA.5 escape antibodies elicited by Omicron infection. Nature 608 (7923), 593–602. https://doi.org/10.1038/s41586-022-04980-y.

Chong, H., Wu, X., Su, Y., He, Y., 2016. Development of potent and long-acting HIV-1 fusion inhibitors. AIDS 30, 1187–1196.

Chong, H., Xue, J., Xiong, S., Cong, Z., Ding, X., Zhu, Y., et al., 2017. A lipopeptide HIV-1/2 fusion inhibitor with highly potent in vitro, ex vivo, and in vivo antiviral activity. J. Virol. 91 e00288-00217.

Chong, H., Zhu, Y., Yu, D., He, Y., 2018a. Structural and functional characterization of membrane fusion inhibitors with extremely potent activity against HIV-1, HIV-2, and simian immunodeficiency virus. J. Virol. 92 e01088-01018.

Chong, H., Xue, J., Zhu, Y., Cong, Z., Chen, T., Guo, Y., et al., 2018b. Design of novel HIV-1/2 fusion inhibitors with high therapeutic efficacy in rhesus monkey models. J. Virol. 92 e00775-00718.

Chong, H., Xue, J., Zhu, Y., Cong, Z., Chen, T., Wei, Q., et al., 2019. Monotherapy with a low-dose lipopeptide HIV fusion inhibitor maintains long-term viral suppression in rhesus macaques. PLoS Pathog. 15, e1007552.

Ding, X., Zhang, X., Chong, H., Zhu, Y., Wei, H., Wu, X., et al., 2017. Enfuvirtide (T20)-based lipopeptide is a potent HIV-1 cell fusion inhibitor: implication for viral entry and inhibition. J. Virol. 91 e00831-00817.

Garcia-Beltran, W.F., Lam, E.C., St Denis, K., Nitido, A.D., Garcia, Z.H., Hauser, B.M., et al., 2021. Multiple SARS-CoV-2 variants escape neutralization by vaccine-induced humoral immunity. Cell 184, 2372–2383 e2379.

Guo, Y., Han, J., Zhang, Y., He, J., Yu, W., Zhang, X., et al., 2022. SARS-CoV-2 Omicron variant: epidemiological features, biological characteristics, and clinical significance. Front. Immunol. 13, 877101.

He, X., Hong, W., Pan, X., Lu, G., Wei, X., 2020. SARS-CoV-2 Omicron variant: characteristics and prevention. MedComm 2021.

Hoffmann, M., Arora, P., Gross, R., Seidel, A., Hornich, B.F., Hahn, A.S., et al., 2021. SARS-CoV-2 variants B.1.351 and P.1 escape from neutralizing antibodies. Cell 184, 2384–2393 e2312.

Korber, B., Fischer, W.M., Gnanakaran, S., Yoon, H., Theiler, J., Abfalterer, W., et al., 2020. Tracking changes in SARS-CoV-2 spike: evidence that D614G increases infectivity of the COVID-19 virus. Cell 182, 812–827 e819.

Kuzmina, A., Khalaila, Y., Voloshin, O., Keren-Naus, A., Boehm-Cohen, L., Raviv, Y., et al., 2021. SARS-CoV-2 spike variants exhibit differential infectivity and neutralization resistance to convalescent or post-vaccination sera. Cell Host Microbe 29, 522–528 e522.

Lan, Q., Chan, J.F., Xu, W., Wang, L., Jiao, F., Zhang, G., et al., 2022. A palmitic acid-conjugated, peptide-based pan-CoV fusion inhibitor potently inhibits infection of SARS-CoV-2 Omicron and other variants of concern. Viruses 14, 549.

Lee, K.K., Pessi, A., Gui, L., Santoprete, A., Talekar, A., Moscona, A., et al., 2011. Capturing a fusion intermediate of influenza hemagglutinin with a cholesterol-conjugated peptide, a new antiviral strategy for influenza virus. J. Biol. Chem. 286, 42141–42149.

Li, Q., Wu, J., Nie, J., Zhang, L., Hao, H., Liu, S., et al., 2020. The impact of mutations in SARS-CoV-2 spike on viral infectivity and antigenicity. Cell 182, 1284–1294 e1289.

Lin, X., Guo, L., Lin, S., Chen, Z., Yang, F., Yang, J., et al., 2022. An engineered 5-helix bundle derived from SARS-CoV-2 S2 pre-binds sarbecoviral spike at both serological- and endosomal-pH to inhibit virus entry. Emerg. Microb. Infect. 11, 1920–1935.

Markov, P.V., Katzourakis, A., Stilianakis, N.I., 2022. Antigenic evolution will lead to new SARS-CoV-2 variants with unpredictable severity. Nat. Rev. Microbiol. 20, 251–252.

Qu, P., Faraone, J., Evans, J.P., Zou, X., Zheng, Y.M., Carlin, C., et al., 2022. Neutralization of the SARS-CoV-2 Omicron BA.4/5 and BA.2.12.1 subvariants. N. Engl. J. Med. 386, 2526–2528.

Saito, A., Irie, T., Suzuki, R., Maemura, T., Nasser, H., Uriu, K., et al., 2022. Enhanced fusogenicity and pathogenicity of SARS-CoV-2 Delta P681R mutation. Nature 602, 300–306.

Schmitz, K.S., Geers, D., de Vries, R.D., Bovier, T.F., Mykytyn, A.Z., Geurts van Kessel, C. H., et al., 2022. Potency of fusion-inhibitory lipopeptides against SARS-CoV-2 variants of concern. mBio 13, e0124922.

Tang, T., Bidon, M., Jaimes, J.A., Whittaker, G.R., Daniel, S., 2020. Coronavirus membrane fusion mechanism offers a potential target for antiviral development. Antivir. Res. 178, 104792.

Tao, K., Tzou, P.L., Nouhin, J., Gupta, R.K., de Oliveira, T., Kosakovsky Pond, S.L., et al., 2021. The biological and clinical significance of emerging SARS-CoV-2 variants. Nat. Rev. Genet. 22, 757–773.

Tegally, H., Moir, M., Everatt, J., Giovanetti, M., Scheepers, C., Wilkinson, E., et al., 2022. Emergence of SARS-CoV-2 Omicron lineages BA.4 and BA.5 in South Africa. Nat. Med.

Ujike, M., Nishikawa, H., Otaka, A., Yamamoto, N., Yamamoto, N., Matsuoka, M., et al., 2008. Heptad repeat-derived peptides block protease-mediated direct entry from the cell surface of severe acute respiratory syndrome coronavirus but not entry via the endosomal pathway. J. Virol. 82, 588–592.

Walls, A.C., Park, Y.J., Tortorici, M.A., Wall, A., McGuire, A.T., Veesler, D., 2020. Structure, function, and antigenicity of the SARS-CoV-2 spike glycoprotein. Cell 181, 281–292 e286.

Wrapp, D., Wang, N., Corbett, K.S., Goldsmith, J.A., Hsieh, C.L., Abiona, O., et al., 2020. Cryo-EM structure of the 2019-nCoV spike in the prefusion conformation. Science 367, 1260–1263.

Xia, S., Chan, J.F., Wang, L., Jiao, F., Chik, K.K., Chu, H., et al., 2022. Peptide-based pan-CoV fusion inhibitors maintain high potency against SARS-CoV-2 Omicron variant. Cell Res. 32, 404–406.

Xing, L., Xu, X., Xu, W., Liu, Z., Shen, X., Zhou, J., et al., 2022. A five-helix-based SARS-CoV-2 fusion inhibitor targeting heptad repeat 2 domain against SARS-CoV-2 and its variants of concern. Viruses 14.

Xue, J., Chong, H., Zhu, Y., Zhang, J., Tong, L., Lu, J., et al., 2022. Efficient treatment and pre-exposure prophylaxis in rhesus macaques by an HIV fusion-inhibitory lipopeptide. Cell 185, 131–144 e118.

Yamasoba, D., Kimura, I., Nasser, H., Morioka, Y., Nao, N., Ito, J., et al., 2022. Virological characteristics of the SARS-CoV-2 Omicron BA.2 spike. Cell 185, 2103–2115 e2119.

Yu, D., Zhu, Y., Jiao, T., Wu, T., Xiao, X., Qin, B., et al., 2021a. Structure-based design and characterization of novel fusion-inhibitory lipopeptides against SARS-CoV-2 and emerging variants. Emerg. Microb. Infect. 10, 1227–1240.

Yu, D., Zhu, Y., Yan, H., Wu, T., Chong, H., He, Y., 2021b. Pan-coronavirus fusion inhibitors possess potent inhibitory activity against HIV-1, HIV-2, and simian immunodeficiency virus. Emerg. Microb. Infect. 10, 810–821.

Zeng, C., Evans, J.P., King, T., Zheng, Y.M., Oltz, E.M., Whelan, S.P.J., et al., 2022. SARS-CoV-2 spreads through cell-to-cell transmission. Proc. Natl. Acad. Sci. U. S. A. 119.

Zhang, J., Xiao, T., Cai, Y., Lavine, C.L., Peng, H., Zhu, H., et al., 2021. Membrane fusion and immune evasion by the spike protein of SARS-CoV-2 Delta variant. Science 374, 1353–1360.

Zhao, H., Lu, L., Peng, Z., Chen, L.L., Meng, X., Zhang, C., et al., 2022. SARS-CoV-2 Omicron variant shows less efficient replication and fusion activity when compared with Delta variant in TMPRSS2-expressed cells. Emerg. Microb. Infect. 11, 277–283.

Zhu, Y., Zhang, X., Ding, X., Chong, H., Cui, S., He, J., et al., 2018. Exceptional potency and structural basis of a T1249-derived lipopeptide fusion inhibitor against HIV-1, HIV-2, and simian immunodeficiency virus. J. Biol. Chem. 293, 5323–5334.

Zhu, Y., Chong, H., Yu, D., Guo, Y., Zhou, Y., He, Y., 2019. Design and characterization of cholesterylated peptide HIV-1/2 fusion inhibitors with extremely potent and long-lasting antiviral activity. J. Virol. 93 e02312-02318.

Zhu, Y., Yu, D., Yan, H., Chong, H., He, Y., 2020. Design of potent membrane fusion inhibitors against SARS-CoV-2, an emerging coronavirus with high fusogenic activity. J. Virol. 94 e00635-00620.

Zhu, Y., Yu, D., Hu, Y., Wu, T., Chong, H., He, Y., 2021. SARS-CoV-2-derived fusion inhibitor lipopeptides exhibit highly potent and broad-spectrum activity against divergent human coronaviruses. Signal Transduct. Targeted Ther. 6, 294.

Zhu, Y., Dong, X., Liu, N., Wu, T., Chong, H., Lei, X., et al., 2022. SARS-CoV-2 fusion-inhibitory lipopeptides maintain high potency against divergent variants of concern including Omicron. Emerg. Microb. Infect. 11, 1819–1827.